European Journal of Medicinal Chemistry 92 (2015) 191–201

Contents lists available at ScienceDirect

European Journal of Medicinal Chemistry

journal homepage: http://www.elsevier.com/locate/ejmech

Original article

Development of certain novel *N*-(2-(2-(2-oxoindolin-3-ylidene) hydrazinecarbonyl)phenyl)-benzamides and 3-(2-oxoindolin-3-ylideneamino)-2-substituted quinazolin-4(3*H*)-ones as CFM-1 analogs: Design, synthesis, QSAR analysis and anticancer activity

Ahmed M. Alafeefy [a, *], Abdelkader E. Ashour [b], Onkar Prasad [c], Leena Sinha [c], Shilendra Pathak [c], Fatimah A. Alasmari [d], Arun K. Rishi [e, f, g], Hatem A. Abdel-Aziz [h, i, **]

[a] Department of Pharmaceutical Chemistry, College of Pharmacy, Salman Bin Abdulaziz University, P.O. Box 173, Alkharj, 11942, Saudi Arabia
[b] Department of Pharmacology and Toxicology, College of Pharmacy, King Saud University, P.O. Box 2457, Riyadh, 11451, Saudi Arabia
[c] Department of Physics, University of Lucknow, 226007, Lucknow, India
[d] Department of Chemistry, College of Science, King Saud University, PO Box 22955, Riyadh, 11416, Saudi Arabia
[e] John D. Dingell VA Medical Center, Wayne State University, Detroit, MI, USA
[f] Karmanos Cancer Institute, Wayne State University, Detroit, MI, USA
[g] Department of Oncology, Wayne State University, Detroit, MI, USA
[h] Department of Pharmaceutical Chemistry, College of Pharmacy, King Saud University, P.O. Box 2457, Riyadh, 11451, Saudi Arabia
[i] Department of Applied Organic Chemistry, National Research Center, Dokki, Cairo, 12622, Egypt

ARTICLE INFO

Article history:
Received 1 November 2014
Received in revised form
25 December 2014
Accepted 26 December 2014
Available online 27 December 2014

Keywords:
Hydrazones
Quinazoline
2-oxoindolin-3-ylidene
CFM analogues
Anticancer agents

ABSTRACT

The reaction of *N*-(2-(hydrazinecarbonyl)aryl)benzamides **2a**, **b** with indoline-2,3-diones **4ae** in acidified ethanolic solution furnished the corresponding *N*-(2-(2-(2-oxoindolin-3-ylidene)hydrazinecarbonyl) phenyl)benzamides **5aj**, respectively. Furthermore, 3-(2-oxoindolin-3-ylideneamino)-2-substituted quinazolin-4(3*H*)-ones **6aj** were prepared by the reaction of 3-amino-2-arylquinazolin-4(3*H*)-one **3a**, **b** with **4ae**. Six derivatives of the twenty newly synthesized compounds showed remarkable antitumor activity against most of the tested cell lines, Daoy, UW228-2, Huh-7, Hela and MDA-MB231. Although these six compounds were more potent than the standard drug (CFM-1), indeed compounds **5b**, **5d** and **6b** were the best candidates with IC_{50} values in the range 1.866.87, 4.4210.89 and 1.468.60 μg/ml and percentage inhibition in the range 77.188.7, 59.4184.8 and 75.488.0%, respectively. QSAR analyses on the current series of derivatives also have been performed for all five cancer cell lines and thus 10 statistically significant models were developed and internally cross validated.

1. Introduction

Cancer is a major health problem which concerns the medical community all over the world. In spite of the substantial progress in many aspects of cancer research, cancer chemotherapy is highly inadequate [1]. Quinazolin-4(3*H*)-one containing molecules constitute an important category among heterocyclic compounds of medical, technological and industrial interest [2]. They have attracted researchers' interest owing to their diverse biological activities, particularly as enzyme inhibitors, receptor agonists and antagonists, as well as antiviral activities. Derivatives such as PD153035 and gefitinib (Scheme 1) were described to selectively inhibit EGFR, notably on cellular assays and the isolated receptors [3], they do not directly inhibit other ErbB receptors [4]. Additionally, they were found to down-regulate the phosphorylation of EGFR and consequently suppress the proliferation of human cancer cell lines under conditions of overexpression of EGFR [5–7]. That is why EGFR inhibitors are considered to be highly useful in the treatment of several malignancies. This was supported and evidenced by several clinical studies which have revealed the potential use of these small molecules in the treatment of ovarian and cervical cancer, both in the frontline and in the recurrent setting [8].

* Corresponding author.
** Corresponding author. Department of Pharmaceutical Chemistry, College of Pharmacy, King Saud University, P.O. Box 2457, Riyadh, 11451, Saudi Arabia.
E-mail addresses: a.alafeefy@sau.edu.sa (A.M. Alafeefy), hatem_741@yahoo.com (H.A. Abdel-Aziz).

http://dx.doi.org/10.1016/j.ejmech.2014.12.048
0223-5234/

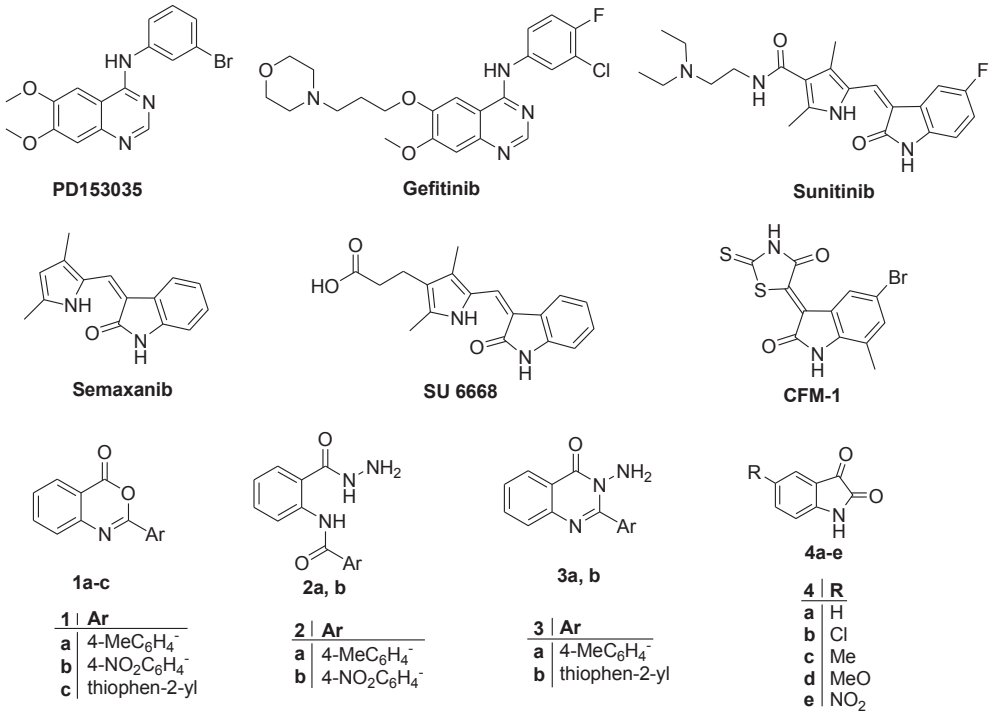

Scheme 1. Structure of compounds PD153035, gefitinib, sunitinib, semaxanib, SU 6668, CFM-1 and **1**–**4**.

These facts show that other quinazoline derivatives are eligible for in vitro and in vivo antitumor testing and might be helpful for cancer treatment [3].

In addition, there are many reports on oxoindole derivatives as potential antitumor and cytotoxic agents; these include Sunitinib [9,10], Semaxanib [11,12], and SU 6668 [13], (Scheme 1). Recently, certain indolin-2-one derivatives were reported as multitargeted receptor-tyrosine kinase inhibitors which effectively inhibited members of both the VEGFR and PDGFR families, each of which plays a major role in angiogenesis. Some of these compounds were low nanomolar inhibitors of the enzyme activity; the structure activity co-relation and the virtual docking studies intensify the importance and interest of these compounds [3].

Rishi et al. identified and characterized a peri-nuclear phosphoprotein, termed CARP-1/CCAR1. It was considered as a cell cycle regulator and a key transducer of cell growth [14–16]. The function of CARP-1 was recently exploited to recognize a number of inhibitors coined CARP-1 Functional Mimetics (CFMs) (Scheme 1) which suppress the growth of a range of cancer cells in part by stimulating apoptosis [17].

Based on the aforementioned facts, we synthesized novel 20 CFM-1 analogues **5a**–**j** and **6a**–**j** by the reaction of **4a**–**e** with **2a, b** or **3a, b**, respectively, and tested their cytotoxic activities. We report here the percentage growth inhibition, as well as the IC_{50} values of these analogues along, with CFM-1, as a standard drug, against five tumor cell lines.

Quantitative structure–activity relationship (QSAR) is among the most practical tool in computational chemistry. The fundamental idea of QSAR consists of the possibility of relationships between a set of descriptors, which are derived from molecular structure and a molecular response. QSAR can be regarded as a computer-derived rule that quantitatively describes the biological activity in terms of chemical descriptors; it has been frequently used to predict biological activities of new compounds [18]. In the present study, QSAR analysis on synthesized ten *N*-(2-(2-(2-oxoindolin-3-ylidene)hydrazinecarbonyl)phenyl)benzamides **5a**–**j** and ten 3-(2-oxoindolin-3-ylideneamino)-2-substituted quinazolin-4(3*H*)-one derivatives **6a**–**j** have been performed to develop statistically significant models, so that in future these can be used to predict and synthesize new derivatives having remarkable biological inhibition activity.

2. Results and discussion

2.1. Chemistry

Benzamide derivatives **2a**, **b** were prepared by the reaction of 2-methyl-4*H*-benzo[d][1,3]oxazin-4-ones **1a**, **b** with hydrazine hydrate in ethanol while 3-amino-2-arylquinazolin-4(3*H*)-ones **3a**, **b** were obtained by the reaction of **1a**, **c** with hydrazine hydrate using *n*-butanol instead of ethanol [1] (Scheme 2).

The newly synthesized compounds *N*-(2-(2-(2-oxoindolin-3-ylidene)hydrazinecarbonyl)phenyl)benzamides **5a**–**j** were prepared by the reaction of *N*-(2-(hydrazinecarbonyl)aryl)benzamides **2a**, **b** with indoline-2,3-dione **4a**–**e** in acidified ethanolic solution (Scheme 2). Similarly, the new 3-(2-oxoindolin-3-ylideneamino)-2-substituted quinazolin-4(3*H*)-ones **6a**–**j** were prepared by the reaction of 3-amino-2-arylquinazolin-4(3*H*)-one **3a**, **b** with indoline-2,3-dione **4a**–**e** (Scheme 2).

2.2. Antitumor testing

Thirteen compounds showed varying degrees of remarkable antitumor activities at the micromolar range (Table 1). Three of them namely, **5b**, **5d** and **6b** were highly effective against the five tumor cell lines, Daoy, UW228-2, Huh-7, Hela and MDA-MB231 with IC_{50} values in the range 1.86–6.87, 4.42–10.89 and 1.46–8.60 μg/ml and percentage inhibition in the range 77.1–88.7, 59.41–84.8 and 75.4–88.0%, respectively. Compounds **6d** and **6i** showed good activity against four tumor cell lines, Daoy, UW228-2,

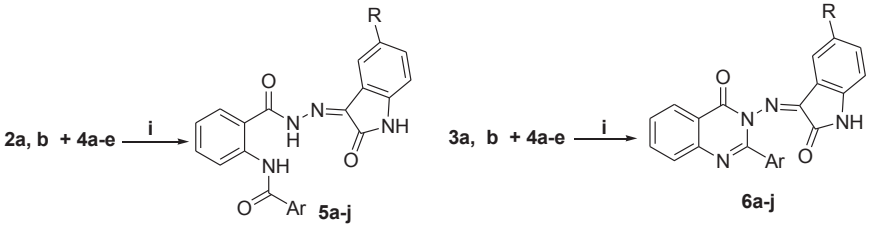

5	R	Ar
a	H	4-MeC_6H_4
b	Cl	4-MeC_6H_4
c	Me	4-MeC_6H_4
d	MeO	4-MeC_6H_4
e	NO_2	4-MeC_6H_4
f	H	4-$NO_2C_6H_4$
g	Cl	4-$NO_2C_6H_4$
h	Me	4-$NO_2C_6H_4$
i	MeO	4-$NO_2C_6H_4$
j	NO_2	4-$NO_2C_6H_4$

6	R	Ar
a	H	4-MeC_6H_4
b	Cl	4-MeC_6H_4
c	Me	4-MeC_6H_4
d	MeO	4-MeC_6H_4
e	NO_2	4-MeC_6H_4
f	H	thiophen-2-yl
g	Cl	thiophen-2-yl
h	Me	thiophen-2-yl
i	MeO	thiophen-2-yl
j	NO_2	thiophen-2-yl

Scheme 2. Synthesis of the target compounds **5a**–**j** and **6a**–**j**. Reactions and conditions: (i) absolute ethanol/few drops glacial acetic acid/reflux 5–8 h.

Huh-7 and Hela. However, compounds **5a**, **5f** and **5h** were of interesting anti-proliferative properties against three tumor cell lines. Compounds **5e**, **6e**, **6g** and **6h** were active only against two tumor cell lines, whereas **6f** was active only against one tumor cell line (Daoy). On the other hand seven compounds **5c**, **5g**, **5i**, **5j**, **6a**, **6c**, and **6j**, were totally inactive.

Daoy cell line was the most sensitive one; it was inhibited by thirteen compounds followed by Hela cell line, the growth of which was suppressed by nine compounds. UW228-2 and Huh-7 were inhibited by eight compounds. The least sensitive cell line was MDA-MB231 which was sensitive towards three compounds only.

2.3. The structure activity correlation

It is evident that methyl group at position-4 of aryl group in the quinazoline moiety in addition to chlorine atom or methoxy group in isatin moiety is essential for biological activity. Compounds contain the latter substitutions were the most potent compounds with average IC_{50} of ~4.87 μg/ml. However compounds bearing thiophene moiety were less active than the previous ones, but were more potent than those derivatives containing 4-nitrophenyl group at position-2 of the quinazoline nucleus. Thus, we can conclude that phenyl group at position-2 with electron donating substituent at position-4 such as CH_3 has better impact on activity than electron withdrawing group such as NO_2.

2.4. QSAR analysis

2.4.1. Cancer cell inhibitory activity

Logarithmic value of experimentally observed percent inhibition of different cancer cell growth at a concentration of 25 μg/ml (Log % 125 μg/ml) was used as a dependent variable for the development of valid QSAR models.

2.4.2. Computational details

Three dimensional initial structures of considered compounds were constructed by means of Gauss view 5.0.8 program [19], and then their geometries were optimized to find out conformations with least potential energy, using Becke's three parameter hybrid exchange functional [20] with Lee–Yang–Parr correlation functional (B3LYP) [21,22] of DFT and 6–311++G(d,p) basis set with the help of Gaussian 09 software [23].

A diverse set of molecular parameters (over 1660) including different group and class of descriptors as constitutional, walk and path counts, information indices, connectivity indices, topological, radial distribution function (RDF), 2D autocorrelation edge adjacency indices, topological charge indices, eigenvalue-based indices, 3D-MoRSE, WHIM, GATAWAY, functional group counts, charge molecular properties, atom centered fragment etc. were calculated for all compounds using EDRAGON [24] software. Eight QSAR descriptors (surface area approx, surface area grid, volume, hydration energy, log P, polarizability, refractivity and mass) calculated by Hyperchem [25] and 5 descriptors (total energy, energy of HOMO and LUMO, HOMO-LUMO gap and molecular dipole moment) obtained from DFT calculation using Gaussian 09 software, were also included in the analysis.

2.4.3. Statistical analysis

For developing QSAR models, multiple linear regression approach with stepwise selection and elimination of variables was employed. Internal cross-validation technique with leave-one-out (LOO) method [26] was used to verify the statistical significance and predictive ability of the developed models. Statistical software package SPSS 21 [27] has been used for all these propose.

2.4.4. QSAR models

After computing over 1270 structural descriptors for all synthesized compounds, Pearson's correlation matrix has been performed on all descriptors for selection of a set of appropriate descriptors. Analysis of the matrix revealed 15 descriptors for the development of multi linear regression (MLR) models. Stepwise multilinear regression analysis on these 15 molecular descriptors revealed the following 2 and 3 independent parametric statistically significant QSAR equations, for biological activity of *N*-(2-(2-(2-oxoindolin-3-ylidene) hydrazinecarbonyl) phenyl) benzamides **5a**–**j** and 3-(2-oxoindolin-3-ylideneamino)-2-substituted quinazolin-4(3*H*)-ones **6a**–**j** respectively, in terms of structural descriptors:

*A. QSAR equations for inhibitory activities of N-(2-(2-(2-oxoindolin-3-ylidene) hydrazinecarbonyl) phenyl) benzamide **5a**–**j**.*

Model 1 (against Daoy cancer line)

$$Log(\%inhib.) = -4.950 - 0.476*RDF140m + 0.824*SPAN \quad (1)$$

Table 1
In vitro cytotoxicity of compounds **5a–j**, **6a–j** and CFM-1 against selected cancer cell lines.

Comp.	% Inhibition[a]/IC_{50}[b]				
	Daoy	UW228-2	Huh-7	Hela	MDA-MB231
5a	72.8/3.94	71.7/6.06	56.4/5.00	30.4/nt[c]	46.8/nt[c]
5b	77.1/1.86	88.7/6.87	84.1/3.20	86.7/6.52	85.0/5.95
5c	49.1/nt[c]	23.2/nt[c]	38.0/nt[c]	46.5/nt[c]	37.7/nt[c]
5d	77.2/4.42	84.8/5.82	81.6/4.6	80.3/8.09	59.41/10.89
5e	75.8/6.61	38.5/nt[c]	55.2/11.6	26.8/nt[c]	30.2/nt[c]
5f	79.1/2.72	51.8/20.0	48.6/nt[c]	55.0/16.52	44.9/nt[c]
5g	36.6/nt[c]	41.6/nt[c]	43.1/nt[c]	31.0/nt[c]	35.5/nt[c]
5h	62.7/11.86	58.7/9.62	55.8/19.3	46.1/nt[c]	40.8/nt[c]
5i	11.1/nt[c]	24.5/nt[c]	33.2/nt[c]	16.3/nt[c]	34.8/nt[c]
5j	31.9/nt[c]	04.8/nt[c]	08.2/nt[c]	14.7/nt[c]	00.0/nt[c]
6a	41.4/nt[c]	09.3/nt[c]	02.9/nt[c]	42.3/nt[c]	24.7/nt[c]
6b	75.4/1.46	88.0/5.70	83.3/3.76	80.8/8.60	78.1/4.80
6c	47.0/nt[c]	02.1/nt[c]	07.2/nt[c]	42.8/nt[c]	34.3/nt[c]
6d	82.8/3.61	58.9/20.8	53.6/22.8	68.0/9.89	35.36/nt[c]
6e	58.8/11.66	22.8/nt[c]	00.0/nt[c]	52.9/21.15	23.6/nt[c]
6f	69.7/5.4	00.0/nt[c]	00.0/nt[c]	36.2/nt[c]	10.7/nt[c]
6g	69.3/15.68	28.4/nt[c]	00.0/nt[c]	69.7/16.96	06.1/nt[c]
6h	59.4/18.97	32.1/nt[c]	32.9/nt[c]	57.8/19.29	29.5/nt[c]
6i	80.5/3.25	56.4/21.4	62.7/19.93	67.0/11.0	13.6/nt[c]
6j	18.4/nt[c]	00.0/nt[c]	00.0/nt[c]	00.0/nt[c]	00.0/nt[c]
CFM-1	64.8/8.12	51.4/16.4	61.8/8.18	57.6/13.5	52.5/19.7

[a] Percent inhibition of cell survival at a concentration of 25 μg/ml, relative to control.
[b] IC_{50} is expressed as μg/ml.
[c] nt: Not tested.

$$\left(r = 0.959,\ r^2 = 0.919,\ r^2_{adj} = 0.753,\ s = 0.088,\ F = 39.839,\ p < 10^{-3}\right)$$

where RDF140m is Radial Distribution Function − 140/weighted by mass (RDF descriptors) and SPAN is span R Geometrical descriptors.

Model 2 (against UW228-2 cancer line)

$$Log(\%inhib.) = 11.407 - 5.090*EEig12d - 19.265*G1m \quad (2)$$

$$\left(r = 0.930,\ r^2 = 0.864,\ r^2_{adj} = 0.825,\ s = 0.157,\ F = 22.248,\ p < 10^{-3}\right)$$

where ESpm12d is Spectral moment 12 from edge adj. Matrix weighted by dipole moments (Edge adjacency indices) and G1m is 1st component symmetry directional WHIM index/weighed by mass (WHIM descriptors).

Model 3 (against Huh-7 cancer line)

$$Log(\%inhhib.) = -14.070 + 8.025*Ks + 12.509*BIC4 \quad (3)$$

$$\left(r = 0.986,\ r^2 = 0.972,\ r^2_{adj} = 0.964,\ s = 0.054,\ F = 122.190,\ p < 10^{-5}\right)$$

where Ks is K global shape index/weighted by I-state (WHIM descriptors) and BIC4 is Bond Information Content index (neighborhood symmetry of 4-order) (Information indices)

Model 4 (against Hela cancer line)

$$Log(\%inhib.) = -0.023 - 0.012*G(O..O) + 2.517*EEig14d \quad (4)$$

$$\left(r = 0.912,\ r^2 = 0.831,\ r^2_{adj} = 0.783,\ s = 0.122,\ F = 17.238,\ p = 0.001975\right)$$

where G(O..O) is sum of geometrical distances between O..O (3D Atom Pairs) and EEig14d is Eigenvalue 14 from edge adj. matrix weighted by dipole moments

Model 5 (against MDA-MB231cancer line)

$$Log\ (\%inhib.) = 38.611 - 14.624*EEig13x - 0.629*GATS6m \quad (5)$$

$$\left(r = 0.993,\ r^2 = 0.985,\ r^2_{adj} = 0.981,\ s = 0.073,\ F = 235.462,\ p < 10^{-6}\right)$$

where EEig13x is Eigenvalue 13 from edge adj. matrix weighted by edge degrees (Edge adjacency indices), GATS6m − Geary autocorrelation of lag 6 weighted by mass (2D autocorrelations).

B. QSAR equations for inhibitory activities of fifteen 3-(2-oxoindolin-3-ylideneamino)-2-substituted quinazolin-4(3H)-one ***6a–j.***

Model 6 (for cancer line Daoy)

$$\text{Log}(\%\ \text{inhib.}) = 5.687 + 1.810*GATS1v - 32.457*G2v \quad (6)$$

$$\left(N = 10,\ r = 0.945,\ r^2 = 0.893,\ r^2_{adj} = 0.863,\ s = 0.726,\ F = 29.247,\ p < 10^{-3}\right)$$

where GATS1v is Geary autocorrelation of lag 1 weighted by van der Waals volume a 2D autocorrelations descriptor while G2v is 2nd component symmetry directional WHIM index/weighted by van der Waals volume (WHIM descriptors).

Model 7 (for cancer line UW228-2)

$$Log(\%inhib.) = -5.585 + 6.923*EEig07d - 5.568*EEig.09d \quad (7)$$

$$\left(N = 10,\ r = 0.966,\ r^2_{adj} = 0.933,\ r^2 = 0.914,\ s = 0.218,\ F = 49.061,\ p < 10^{-4}\right)$$

where EEig07d (Eigenvalue 07 from edge adj. matrix weighted by dipole moments) and EEig09d (Eigenvalue 09 from edge adj. matrix weighted by dipole moments) are Edge adjacency indices

Model 8 (for cancer line Huh-7)

$$Log(\%inhib.) = -21.933 + 17.021*BELm5 + 3.863*MATS5m \quad (8)$$

$$\left(N = 10,\ r = 0.950,\ r^2 = 0.902,\ r^2_{adj} = 0.874,\ s = 0.297,\ F = 32.170,\ p < 10^{-3}\right)$$

where BELm5 (lowest eigenvalue n. 5 of Burden matrix/weighted by atomic masses) is a Burden eigenvalue descriptors and MATS5m (Moran autocorrelation of lag 5 weighted by mass) is a 2D autocorrelations.

Model 9 (for cancer line Hela)

$$Log(\%inhib.) = 11.569 - 255.131*R4e^{+} + 22.995*HATS7m \quad (9)$$

$$\left(N = 10,\ r = 0.981,\ r^2 = 0.962,\ r^2_{adj} = 0.951,\ s = 0.125,\ F = 88.441,\ p < 10^{-4}\right)$$

where R4e+ (R maximal autocorrelation of lag 4/weighted by Sanderson electronegativity) and HATS7m (leverage-weighted autocorrelation of lag 7/weighted by mass) both are GETAWAY descriptors.

Model 10 (for cancer line MDA-MB231)

$$Log(\%inhib.) = 8.157 - 116.618*R4e^{+} - 0.778*GATS3m \quad (10)$$

$$\left(N = 10,\ r = 0.985,\ r^2 = 0.970,\ r^2_{adj} = 0.850,\ s = 0.961,\ F = 111.434,\ p < 10^{-4}\right)$$

where R4e+ (R maximal autocorrelation of lag 4/weighted by Sanderson electronegativity) is a GETAWAY descriptors while GATS3m (Geary autocorrelation of lag 3 weighted by mass) is a 2D autocorrelations.

Several statistical parameters such as regression coefficient(r), square correlation coefficient (r^2), adjusted square correlation coefficient (r^2_{adj}), standard error of estimate (S), value of Fischer's value (F) and significance level (p) < 0.005 are used to check the credibility of developed models. Large value of F, small S, very small p-value, as well as r and r^2 close to one indicates a good QSAR model. In present study, all of developed QSAR models are statistically significant with significance level being (p) < 10^{-3}. The values of multiple correlation coefficient (r) and square correlation coefficient (r^2) which are greater than 0.92 and 0.83 respectively, supports the estimated ability of all QSAR models (Eqs. (1)–(10)).

Predicted activity of all compounds, against cancer lines under consideration, from developed QSAR models along with observed inhibition, are collected in Tables 2 and 3. The correlation plots between experimental and the predicted data from the derived multiple regression QSAR Eqs. (1)–(10) given in Figs. 1–10, indicates that predicted values are much closer to the experimental one. It indicates that developed models can be successfully applied to predict percent inhibition of *N*-(2-(2-(2-oxoindolin-3-ylidene) hydrazinecarbonyl)phenyl)benzamides **5a**–**j** and 3-(2-oxoindolin-3-ylideneamino)-2-substituted quinazolin-4(3*H*)-ones **6a**–**j** against cancer cell lines Daoy, UW228-2, Huh-7, Hela and MDA-MB231.

Determination of predictive ability of the developed model needs validation. To estimate the prediction ability of model by means of internal validation procedures, cross validation approach was conducted. In order to test the validity of the predictive power of selected MLR models, the leave-one-out technique (*LOO* technique) was used. The developed models were validated by calculation of the following statistical parameters: predicted residual sum of squares (PRESS), total sum of squares deviation (SSD) and cross-validated correlation coefficients r^2_{cv} (Table 4).

PRESS is an important cross-validation parameter, as it is a good approximation of the real predictive error of the models. Its value being less than sum of squares deviation (SSD) points out that model predicts better than chance and can be considered statically significant. Smaller PRESS value means better model predictability. The results depicted in Table 4, confirm that all models are statistically significant.

The predictive ability of all models is also sustained by the leave-one-out cross validation, square correlation coefficients ($r^2_{loo\text{-}cv}$) which is in range 0.456–0.976 for developed models. The high and closer value of $r^2_{loo\text{-}cv}$ and r^2 are essential criteria for the best qualification of the QSAR. Cross validation parameters indicates that QSAR models 3–10 have the most predictive ability while models 1 and 2 have the least.

Table 2
Observed, converted and predicted inhibition activity of **5a**–**j** against Daoy, UW228-2, Huh-7, Hela and MDA-MB231cancer cell lines.

Comp.	Daoy				UW228-2				Huh-7			
	% Inhib.	Obs. act. Log(%Inhib.)	Pred. act. Eq. (1)	Res.	% Inhib.	Obs. act. Log(% Inhib.)	Pred. act. Eq. (2)	Res.	% Inhib.	Obs. act. Log(% Inhib.)	Pred. act. Eq. (3)	Res.
5a	72.800	1.862	1.858	0.004	71.700	1.856	1.882	−0.026	56.400	1.751	1.819	−0.068
5b	77.100	1.887	1.909	−0.022	88.700	1.948	1.811	0.137	84.100	1.925	1.977	−0.052
5c	49.100	1.691	1.838	−0.147	23.200	1.365	1.503	−0.138	38.000	1.580	1.603	−0.023
5d	77.200	1.888	1.891	−0.003	84.800	1.928	1.671	0.257	81.600	1.912	1.830	0.082
5e	75.800	1.880	1.903	−0.023	38.500	1.585	1.774	−0.189	55.200	1.742	1.748	−0.006
5f	79.100	1.898	1.842	0.056	51.800	1.714	1.776	−0.062	48.600	1.687	1.630	0.057
5g	36.600	1.563	1.510	0.053	41.600	1.619	1.502	0.117	43.100	1.634	1.619	0.015
5h	62.700	1.797	1.653	0.144	58.700	1.769	1.754	0.015	55.800	1.747	1.708	0.039
5i	11.100	1.045	1.109	−0.064	24.500	1.389	1.514	−0.125	33.200	1.521	1.549	−0.028
5g	31.900	1.504	1.512	−0.008	4.800	0.681	0.670	0.011	8.200	0.914	0.928	−0.014

Comp.	Hela				MDA-MB231			
	%Inhib.	Obs. act. Log(%Inhib.)	Pred. act. Eq. (4)	Res.	%Inhib.	Obs. act. Log(%Inhib.)	Pred. act. Eq. (5)	Res.
5a	30.400	1.483	1.566	−0.083	46.800	1.670	1.720	−0.050
5b	86.700	1.938	1.847	0.091	85.000	1.929	1.881	0.048
5c	46.500	1.667	1.618	0.049	37.700	1.576	1.601	−0.025
5d	80.300	1.905	1.963	−0.058	59.400	1.774	1.756	0.018
5e	26.800	1.428	1.610	−0.182	30.200	1.480	1.509	−0.029
5f	55.000	1.740	1.607	0.133	44.900	1.652	1.562	0.090
5g	31.000	1.491	1.608	−0.117	35.500	1.550	1.641	−0.091
5h	46.100	1.664	1.607	0.057	40.800	1.611	1.511	0.100
5i	16.300	1.212	1.370	−0.158	34.800	1.542	1.611	−0.069
5g	14.700	1.167	1.147	0.020	1.000	0.000	0.003	−0.003

%Inhib.-Percent inhibition of cell survival at a concentration of 25 mg/ml, relative to control.

Table 3
Observed, converted and predicted inhibition activity of **6a–j** against Daoy, UW228-2, Huh-7, Hela and MDA-MB231cancer cell lines.

Comp.	Daoy				UW228-2				Huh-7			
	% Inhib.	Obs. act. Log(%Inhib.)	Pred. act. Eq. (6)	Res.	% Inhib.	Obs. act. Log(% Inhib.)	Pred. act. Eq. (7)	Res.	% Inhib.	Obs. act. Log(% Inhib.)	Pred. act. Eq. (8)	Res.
6a	41.400	1.617	1.600	0.017	9.300	0.968	1.175	−0.207	2.900	0.462	0.362	0.100
6b	75.400	1.877	1.954	−0.077	88.000	1.944	1.859	0.085	83.300	1.921	1.633	0.287
6c	47.000	1.672	1.694	−0.022	2.100	0.322	0.620	−0.298	7.200	0.857	0.551	0.306
6d	82.800	1.918	1.918	0.000	58.900	1.770	1.798	−0.028	53.600	1.729	1.522	0.207
6e	58.800	1.769	1.686	0.083	22.800	1.358	1.446	−0.088	1.000	0.000	0.567	−0.567
6f	69.700	1.843	1.781	0.062	1.000	0.000	0.096	−0.096	1.000	0.000	0.024	−0.024
6g	69.300	1.841	1.777	0.064	28.400	1.453	1.534	−0.081	1.000	0.000	−0.025	0.025
6h	59.400	1.774	1.874	−0.100	32.100	1.507	1.263	0.244	32.900	1.517	1.687	−0.170
6i	80.500	1.906	1.872	0.034	56.400	1.751	1.534	0.217	62.700	1.797	1.988	−0.191
6j	18.400	1.265	1.329	−0.064	1.000	0.000	−0.250	0.250	1.000	0.000	−0.027	0.027

Comp.	Hela				MDA-MB231			
	%Inhib.	Obs. act. Log(%Inhib.)	Pred. act. Eq. (9)	Res.	%Inhib.	Obs. act. Log(%Inhib.)	Pred. act. Eq. (10)	Res.
6a	42.300	1.626	1.524	0.102	24.700	1.393	1.358	0.034
6b	80.800	1.907	2.078	−0.171	78.100	1.893	1.837	0.056
6c	42.800	1.631	1.666	−0.035	34.300	1.535	1.601	−0.066
6d	68.000	1.833	1.896	−0.063	35.360	1.549	1.662	−0.113
6e	52.900	1.723	1.634	0.089	23.600	1.373	1.208	0.165
6f	36.200	1.559	1.508	0.051	10.700	1.029	0.956	0.073
6g	69.700	1.843	1.922	−0.079	6.100	0.785	0.918	−0.133
6h	57.800	1.762	1.770	−0.008	29.500	1.470	1.426	0.044
6i	67.000	1.826	1.628	0.198	13.600	1.134	1.185	−0.051
6j	1.000	0.000	0.088	−0.088	1.000	0.000	0.005	−0.005

%Inhib.-Percent inhibition of cell survival at a concentration of 25 μg/ml, relative to control.

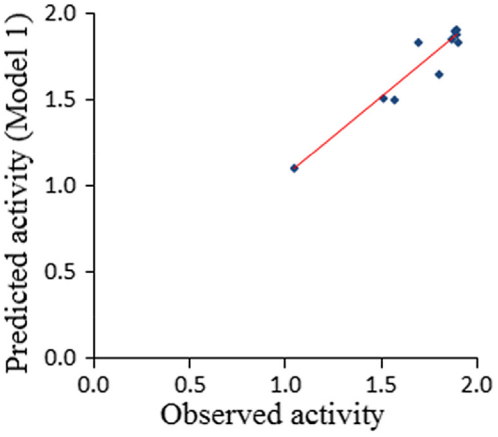

Fig. 1. Observed versus predicted activity for model 1.

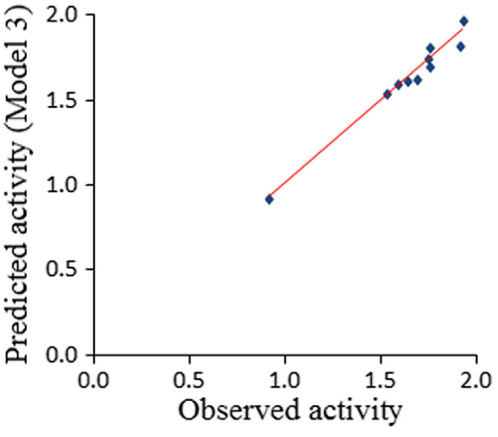

Fig. 3. Observed versus predicted activity for model 3.

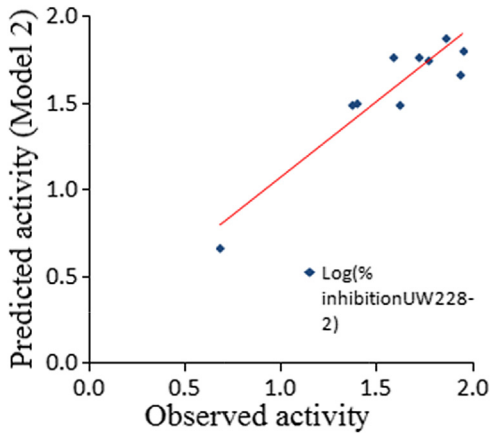

Fig. 2. Observed versus predicted activity for model 2.

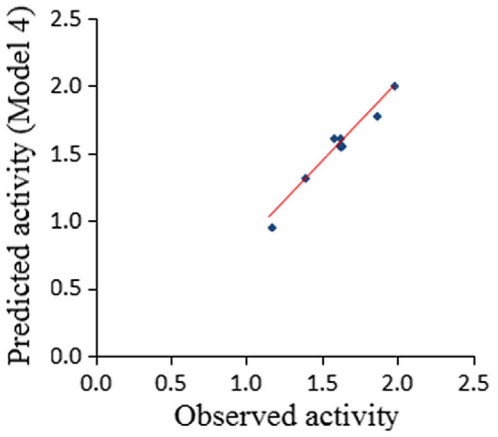

Fig. 4. Observed versus predicted activity for model 4.

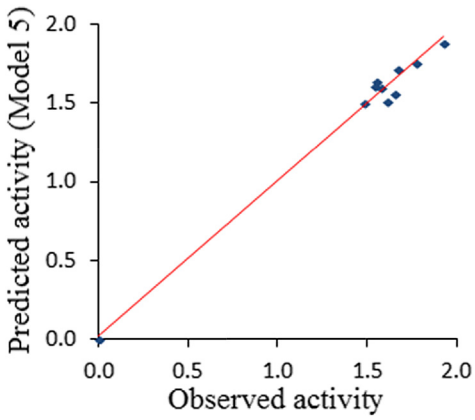

Fig. 5. Observed versus predicted activity for model 5.

3. Conclusion

In conclusion, we prepared twenty novel quinazoline derivatives structurally similar to CFM-1 and tested them against five tumor cell lines. Six compounds showed interesting activity better than the standard drug against most of the tested cancer cell lines. Compound **5b**, **5d** and **6b** were the most potent with IC_{50} values in the range 1.86–6.87, 4.42–10.89 and 1.46–8.60 μg/ml, and percentage inhibition in the range 77.1–88.7, 59.41–84.8 and 75.4–88.0%, respectively. By QSAR analysis of the target compounds, 10 statistically significant models were developed and internally cross validated.

4. Experimental

4.1. Chemistry

4.1.1. General

Melting points (°C, uncorrected) were determined in open capillaries on a Gallenkamp melting point apparatus (Sanyo Gallenkamp, Southborough, UK) and were uncorrected. Precoated silica gel plates (silica gel 0.25 mm, 60G F254; Merck, Germany) were used for thin layer chromatography, dichloromethane/methanol (9.5:0.5) mixture was used as a developing solvent system and the spots were visualized by ultraviolet light and/or iodine. Infrared spectra were recorded in KBr discs using IR-470 Shimadzu spectrometer (Shimadzu, Tokyo, Japan). ^{1}H NMR spectra were recorded on Bruker AC-300 Ultra Shield NMR spectrometer (δ ppm; Bruker, Flawil, Switzerland) at 300 MHz for ^{1}H and 75 MHz for ^{13}C, using TMS as internal standard and peak multiplicities were designed as follows: s, singlet; d, doublet; t, triplet; m, multiplet. Electron Impact Mass Spectra were recorded on a Shimadzu GC-MS-QP 5000 instrument (Shimadzu, Tokyo, Japan), and the purity of compounds was >95%. Elemental analyses were performed, on Carlo Erba 1108 Elemental Analyzer (Heraeus, Hanau, Germany), at the Micro-analytical Unit, Faculty of Science, Cairo University, Cairo, Egypt, and the found results were within ±0.4% of the theoretical values. N-(2-(Hydrazinecarbonyl)aryl)benzamide **2a**, **b** and 3-amino-2-arylquinazolin-4(3*H*)-one **3a**, **b** were prepared according to the reported method [2].

4.1.2. Synthesis of N-(2-(2-(2-oxoindolin-3-ylidene) hydrazinecarbonyl)phenyl)benzamides ***5a–j***

To a mixture of *N*-(2-(hydrazinecarbonyl)aryl)benzamide **2a**, **b** (1 mmol) and indoline-2,3-dione **4a–e** (1 mmol) in ethanol (25 ml), few drops of glacial acetic acid were added. The reaction mixture was refluxed for 5–8 h, and then cooled to room temperature. The precipitate was filtered and dried. The crude product was crystallized from EtOH/DMF to obtain the target.

*4.1.2.1. (Z)-4-Methyl-N-(2-(2-(2-oxoindolin-3-ylidene)hydrazinecarbonyl)phenyl)benzamide (**5a**).* Yield (63%); m.p. 258–260 °C; IR ν 3342–3301 (3NH), 1692–1668 (3C=O) cm^{-1}; ^{1}H NMR (DSMO-d_6) δ 2.33 (s, 3*H*, CH_3), 7.0–8.36 (m, 12H, ArH); ^{13}C NMR (DSMO-d_6) δ 23.17 (CH_3), 119.59, 123.60, 127.85, 128.27, 129.29, 129.51, 130.04, 130.16, 130.26, 130.39, 132.13, 138.11, 139.89, 145.23, 149.24, 155.09, 157.32, 170.16; MS *m/z* (Rel. Int.) (M^+, 398, 7.0); Anal. ($C_{23}H_{18}N_4O_3$, 398) C, 69.34 (69.05); H, 4.55 (4.78); N, 14.06 (13.75).

*4.1.2.2. (Z)-N-(2-(2-(5-Chloro-2-oxoindolin-3-ylidene)hydrazinecarbonyl)phenyl)-4-methyl benzamide (**5b**).* Yield (66%); m.p. > 300 °C; IR ν 3347–3302 (3NH), 1695–1667 (3C=O) cm^{-1}; ^{1}H NMR (DSMO-d_6) δ 2.32 (s, 3*H*, CH_3), 7.01–8.35 (m, 11H, ArH); ^{13}C NMR (DSMO-d_6) δ 23.5 (CH_3), 119.7, 121.6, 123.6, 123.9, 125.2, 128.3, 128.5, 129.5, 129.9, 130.4, 131.4, 131.7, 133.0, 133.4, 138.1, 142.4, 145.7, 164.2, 164.7, 167.1; MS *m/z* (Rel. Int.) 432 (M^+, 71). Anal. ($C_{23}H_{17}ClN_4O_3$, 432.86) C, 63.82 (63.63); H, 3.96 (4.17); Cl, 8.19 (7.89); N, 12.94 (13.08).

*4.1.2.3. (Z)-4-Methyl-N-(2-(2-(5-methyl-2-oxoindolin-3-ylidene) hydrazinecarbonyl)phenyl) benzamide (**5c**).* Yield (55%); m.p. 282–284 °C; IR ν 3341–3305 (3NH), 1696–1664 (3C=O) cm^{-1}; ^{1}H NMR (DSMO-d_6) δ 2.37 (s, 6H, $2CH_3$), 6.99–8.34 (m, 11H, ArH); ^{13}C NMR (DSMO-d_6) δ 23.9 ($2CH_3$), 118.5, 121.2, 121.6, 123.3, 124.7, 127.5, 127.9, 129.4, 129.9, 131.3, 131.8, 132.3, 133.8, 135.1, 138.6, 141.9, 145.2, 162.8, 163.5, 166.9; MS *m/z* (Rel. Int.) 412 (M^+, 38). Anal. ($C_{24}H_{20}N_4O_3$, 412.44) C, 69.89 (70.09); H, 4.89 (5.13); N, 13.58 (13.29).

*4.1.2.4. (Z)-N-(2-(2-(5-Methoxy-2-oxoindolin-3-ylidene)hydrazinecarbonyl)phenyl)-4-methyl benzamide (**5d**).* Yield (57%); m.p. 254–256 °C; IR ν 3352–3307 (3NH), 1698–1661 (3C=O) cm^{-1}; ^{1}H NMR (DSMO-d_6) δ 2.35 (s, 3*H*, CH_3), 3.82 (s, 3*H*, -OCH_3), 7.0–8.36 (m, 11H, ArH); ^{13}C NMR (DSMO-*d6*) δ 24.2 (CH_3), 55.5 (OCH_3), 114.1, 116.4, 119.0, 121.5, 122.8, 123.5, 124.9, 127.2, 127.7, 129.5, 131.2, 132.5, 132.9, 137.8, 139.4, 142.1, 155.7, 163.0, 164.3, 167.5; MS *m/z* (Rel. Int.) 428 (M^+, 46). Anal. ($C_{24}H_{20}N_4O_4$, 428.44) C, 67.28 (67.02); H, 4.71 (4.85); N, 13.08 (12.82).

*4.1.2.5. (Z)-4-Methyl-N-(2-(2-(5-nitro-2-oxoindolin-3-ylidene) hydrazinecarbonyl)phenyl) benzamide (**5e**).* Yield (61%); m.p. > 300 °C; IR ν 3365–3312 (3NH), 1698–1661 (3C=O) cm^{-1}; ^{1}H NMR (DSMO-d_6) δ 2.33 (s, 3*H*, CH_3), 7.19–8.37 (m, 11H, ArH); ^{13}C NMR (DSMO-d_6) δ 24.7 (CH_3), 119.3, 121.4, 122.7, 123.1, 123.6, 124.4, 124.8, 127.2, 127.6, 129.9, 130.9, 132.3, 132.8, 138.3, 142.0, 145.5, 153.1, 162.7, 163.4, 167.1; MS *m/z* (Rel. Int.) 443 (M^+, 17). Anal. ($C_{23}H_{17}N_5O_5$, 443.41) C, 62.30 (62.11); H, 3.86 (4.04); N, 15.79 (15.58).

*4.1.2.6. (Z)-4-Nitro-N-(2-(2-(2-oxoindolin-3-ylidene)hydrazinecarbonyl)phenyl)benzamide (**5f**).* Yield (65%); m.p. > 300 °C; IR ν 3345–3296 (3NH), 1699–1662 (3C=O) (3NH) cm^{-1}; ^{1}H NMR (DSMO-d_6) δ 7.16–8.37 (m, 12H, ArH); ^{13}C NMR (DSMO-d_6) δ 118.0, 121.2, 121.7, 123.5, 124.7, 127.4, 128.3, 129.7, 131.5, 132.4, 132.9, 137.6, 141.0, 146.5, 152.4, 162.5, 163.7, 167.4; MS *m/z* (Rel. Int.) 429 (M^+, 36). Anal. ($C_{22}H_{15}N_5O_5$, 429.39) C, 62.30 (62.02); H, 3.86 (4.05); N, 15.79 (14.57).

*4.1.2.7. (Z)-N-(2-(2-(5-Chloro-2-oxoindolin-3-ylidene)hydrazinecarbonyl)phenyl)-4-nitro benzamide (**5g**).* Yield (64%); m.p. > 300 °C; IR ν 3348–3294 (3NH), 1699–1661 cm^{-1}; ^{1}H NMR

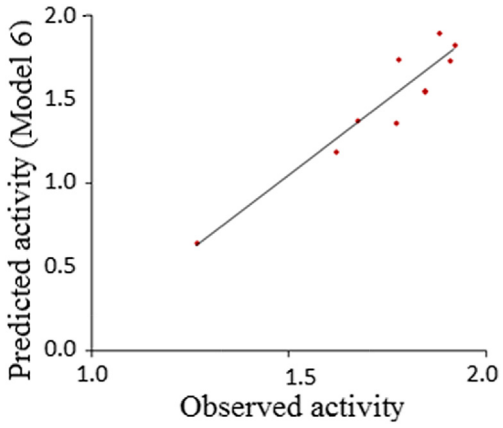

Fig. 6. Observed versus predicted activity for model 6.

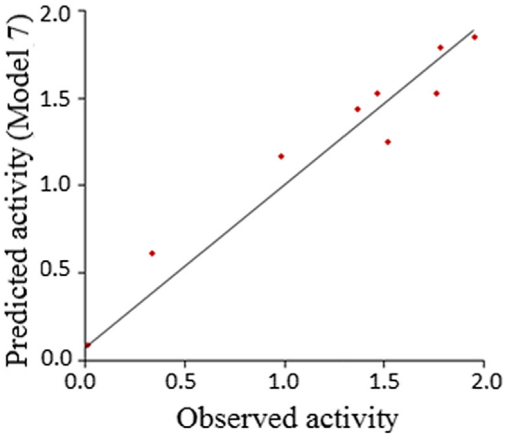

Fig. 7. Observed versus predicted activity for model 7.

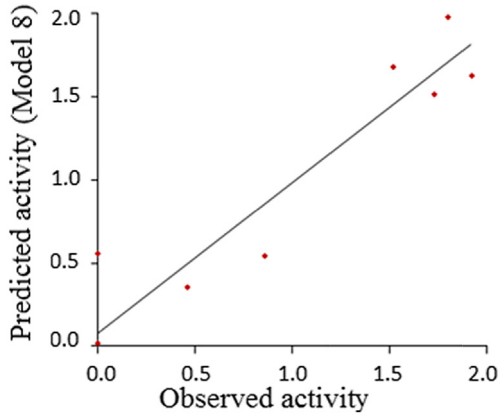

Fig. 8. Observed versus predicted activity for model 8.

(DSMO-d_6) δ 7.17–8.35 (m, 11H, ArH); ^{13}C NMR (DSMO-d_6) δ 118.9, 121.2, 121.6, 123.4, 123.7, 124.5, 127.3, 128.5, 129.3, 130.6, 131.5, 132.3, 132.8, 137.4, 141.7, 144.5, 151.9, 162.8, 163.5, 167.1; MS *m/z* (Rel. Int.) 465 (M^+ + 2, 13), 463 (M^+, 42). Anal. ($C_{22}H_{14}ClN_5O_5$, 463.83) C, 56.97 (57.16); H, 3.04 (3.25); Cl, 7.64 (7.39); N, 15.10 (14.94).

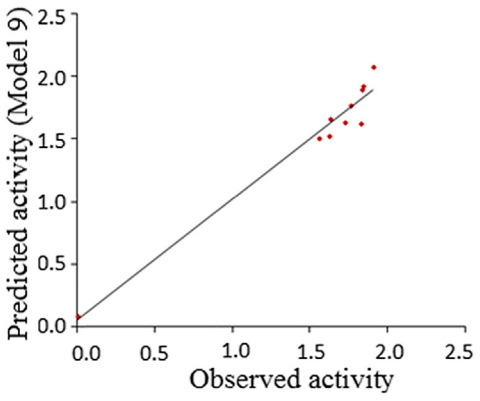

Fig. 9. Observed versus predicted activity for model 9.

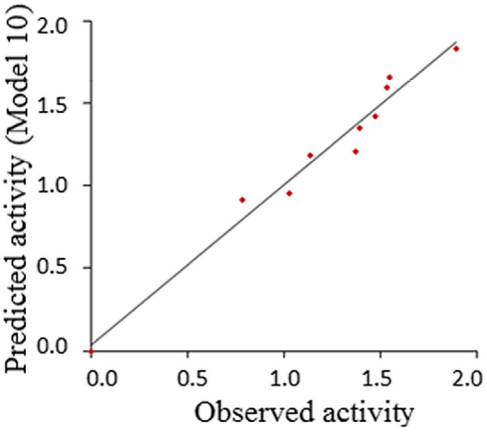

Fig. 10. Observed versus predicted activity for model 10.

Table 4
Cross-validation parameters.

Model no.	PRESS	SSY	PRESS/SSY	$r^2_{-cv-loo}$
1	0.277	0.663	0.417	0.583
2	0.564	1.278	0.441	0.559
3	0.051	0.736	0.069	0.931
4	0.186	0.619	0.301	0.699
5	0.062	2.580	0.024	0.976
6	0.119	0.346	0.344	0.656
7	0.963	4.985	0.193	0.807
8	1.163	6.297	0.185	0.815
9	0.174	2.855	0.061	0.939
10	0.127	2.496	0.051	0.949

*4.1.2.8. (Z)-N-(2-(2-(5-Methyl-2-oxoindolin-3-ylidene)hydrazinecarbonyl)phenyl)-4-nitro benzamide (**5h**).* Yield (59%); m.p. 291–293 °C; IR ν 3347–3290 (3NH), 1705–1662 (3C=O) cm^{-1}; ^{1}H NMR (DSMO-d_6) δ 2.31 (s, 3*H*, CH_3), 7.02–8.37 (m, 11H, ArH); ^{13}C NMR (DSMO-d_6) δ 24.3 (CH_3), 117.5, 121.3, 121.6, 121.9, 123.5, 124.7, 127.6, 128.3, 129.7, 131.5, 132.3, 132.7, 134.6, 137.3, 141.0, 144.6, 152.5, 163.1, 164.9, 167.6; MS *m/z* (Rel. Int.) 443 (M^+, 37).

*4.1.2.9. (Z)-N-(2-(2-(5-Methoxy-2-oxoindolin-3-ylidene)hydrazinecarbonyl)phenyl)-4-nitro benzamide (**5i**).* Yield (54%); m.p. 285–287 °C; IR ν 3353–3291 (3NH), 1703–1665 (3C=O) cm^{-1}; ^{1}H NMR (DSMO-*d6*) δ 3.95 (s, 3*H*, OCH_3), 7.0–8.40 (m, 11H, ArH); ^{13}C NMR (DSMO-d_6) δ 57.7 (OCH_3), 117.5, 121.3, 121.6, 121.9, 123.5, 124.7, 127.6, 128.3, 129.7, 131.5, 132.3, 132.7, 134.6, 137.3, 141.0, 144.6, 152.5,

163.1, 164.9, 167.6; MS *m/z* (Rel. Int.) 459 (M^+, 46). Anal. ($C_{23}H_{17}N_5O_6$, 459.41) C, 60.13 (59.97); H, 3.73 (3.95); N, 15.24 (14.96).

*4.1.2.10. (Z)-4-Nitro-N-(2-(2-(5-nitro-2-oxoindolin-3-ylidene)hydrazinecarbonyl)phenyl) benzamide (**5j**).* Yield (53%); m.p. > 300 °C; IR *ν* 3357–3290 (3NH), 1701–1664 (3C=O) cm^{-1}; ^1H NMR (DSMO-d_6) *δ* 7.02–8.35 (m, 11H, ArH); ^{13}C NMR (DSMO-d_6) *δ* 119.1, 121.4, 121.9, 122.5, 123.3, 123.8, 124.5, 124.7, 127.4, 128.1, 132.6, 132.9, 137.6, 140.8, 144.9, 151.6, 153.0, 162.7, 164.2, 167.5; MS *m/z* (Rel. Int.) 474 (M^+, 28). Anal. ($C_{22}H_{14}N_6O_7$, 474.38) C, 55.70 (55.93); H, 2.97 (3.18); N, 17.72 (17.95).

*4.1.3. Synthesis of 3-(2-oxoindolin-3-ylideneamino)-2-substituted quinazolin-4(3H)-ones **6a–j***

These compounds were prepared following the same procedure for synthesis of compounds **5a–j** by using 3-amino-2-arylquinazolin-4(3*H*)-one **3a**, **b** (1 mmol) instead of hydrazides **2a**, **b**.

*4.1.3.1. (Z)-3-(2-Oxoindolin-3-ylideneamino)-2-p-tolylquinazolin-4(3H)-one (**6a**).* Yield (68%); m.p. > 300 °C; IR *ν* 3289 (NH), 1695, 1675 (2C=O) cm^{-1}; ^1H NMR (DSMO-d_6) *δ* 2.38 (s, 3*H*, CH_3), 7.08–8.08 (m, 12H, ArH); ^{13}C NMR (DSMO-d_6) *δ* 24.6 (CH_3), 118.1, 120.0, 121.6, 123.5, 124.2, 125.2, 126.1, 127.2, 128.6, 129.0, 129.4, 131.3, 132.5, 133.4, 139.7, 146.4, 151.6, 157.1, 161.2, 167.8; MS *m/z* (Rel. Int.) 380 (M^+, 24). Anal. ($C_{23}H_{16}N_4O_2$, 380.40) C, 72.62 (72.47); H, 4.24 (3.98); N, 14.73 (14.55).

*4.1.3.2. (Z)-3-(5-Chloro-2-oxoindolin-3-ylideneamino)-2-p-tolylquinazolin-4(3H)-one (**6b**).* Yield (53%); m.p. > 300 °C; IR *ν* 3288 (NH), 1694, 1667 (2C=O) cm^{-1}; ^1H NMR (DSMO-d_6) *δ* 2.37 (s, 3*H*, CH_3), 7.03–8.12 (m, 11H, ArH); ^{13}C NMR (DSMO-d_6) *δ* 24.6 (CH_3), 119.4, 121.1, 122.1, 123.5, 125.2, 126.1, 127.6, 128.2, 129.3, 129.7, 130.3, 131.5, 132.4, 133.1, 139.5, 145.1, 152.7, 162.0, 166.7; MS *m/z* (Rel. Int.) 414 (M^+, 32). Anal. ($C_{23}H_{15}ClN_4O_2$, 414.84) C, 66.59 (66.75); H, 3.64 (3.46); N, 13.51 (13.27).

*4.1.3.3. (Z)-3-(5-Methyl-2-oxoindolin-3-ylideneamino)-2-p-tolylquinazolin-4(3H)-one (**6c**).* Yield (55%); m.p. 284–286 °C; IR *ν* 3279 (NH), 1701, 1685 (2C=O) cm^{-1}; ^1H NMR (DSMO-d_6) *δ* 2.35 (s, 6H, $2CH_3$), 7.01–8.14 (m, 11H, ArH); ^{13}C NMR (DSMO-d_6) *δ* 24.7 (CH_3), 117.9, 120.6, 121.9, 122.7, 125.4, 126.3, 127.7, 128.4, 129.5, 129.9, 131.4, 132.6, 133.7, 134.3, 140.1, 144.1, 151.5, 159.3, 162.7, 167.3; MS *m/z* (Rel. Int.) 394 (M^+, 13). Anal. ($C_{24}H_{18}N_4O_2$, 394.43) C, 73.08 (72.89); H, 4.60 (4.83); N, 14.20 (13.99).

*4.1.3.4. (Z)-3-(5-Methoxy-2-oxoindolin-3-ylideneamino)-2-p-tolylquinazolin-4(3H)-one (**6d**).* Yield (57%); m.p. 277–79 °C; IR *ν* 3307 (NH), 1703, 1677 (2C=O) cm^{-1}; ^1H NMR (DSMO-d_6) *δ* 2.34 (s, 3*H*, CH_3), 3.81 (s, 3*H*, OCH_3), 6.98–8.16 (m, 11H, ArH); ^{13}C NMR (DSMO-d_6) *δ* 24.7 (CH_3), 57.3 (OCH_3), 114.0, 116.3, 118.7, 120.5, 122.3, 122.7, 125.3, 126.4, 127.5, 128.3, 129.6, 132.7, 133.9, 139.5, 139.7, 151.7, 157.0, 157.9, 162.1, 167.5; MS *m/z* (Rel. Int.) 410 (M^+, 34). Anal. ($C_{24}H_{18}N_4O_3$, 410.42) C, 70.23 (70.05); H, 4.42 (4.16); N, 13.65 (13.41).

*4.1.3.5. (Z)-3-(5-Nitro-2-oxoindolin-3-ylideneamino)-2-p-tolylquinazolin-4(3H)-one (**6e**).* Yield (60%); m.p. > 300 °C; IR *ν* 3291 (NH), 1706, 1675 (2C=O) cm^{-1}; ^1H NMR (DSMO-d_6) *δ* 2.33 (s, 3*H*, CH_3), 7.06–8.17 (m, 11H, ArH); ^{13}C NMR (DSMO-d_6) *δ* 24.3 (CH_3), 118.3, 120.6, 122.1, 122.8, 123.6, 124.2, 125.4, 126.3, 127.4, 128.1, 129.5, 132.3, 133.5, 139.6, 144.0, 151.6, 153.2, 159.7, 161.4, 166.7; MS *m/z* (Rel. Int.) 425 (M^+, 33). Anal. ($C_{23}H_{15}N_5O_4$, 425.40) C, 64.94 (65.17); H, 3.55 (3.29); N, 16.46 (16.70).

*4.1.3.6. (Z)-3-(2-Oxoindolin-3-ylideneamino)-2-(thiophen-2-yl)quinazolin-4(3H)-one (**6f**).* Yield (64%); m.p. 283–285 °C; IR *ν* 3286 (NH), 1701, 1675 (2C=O) cm^{-1}; ^1H NMR (DSMO-d_6) *δ* 7.02–8.14 (m, 11H, ArH), (s, D_2O exchangeable, 1H, NH); ^{13}C NMR (DSMO-d_6) *δ* 118.0, 120.4, 121.7, 122.5, 124.2, 125.3, 126.8, 127.5, 128.3, 129.6, 131.0, 132.2, 133.6, 146.5, 147.1, 159.5, 162.7, 167.2; MS *m/z* (Rel. Int.) 372 (M^+, 26). Anal. ($C_{20}H_{12}N_4O_2S$, 372.40) C, 64.50 (64.27); H, 3.25 (3.49); N, 15.04 (14.85); S, 8.61 (8.34).

*4.1.3.7. (Z)-3-(5-Chloro-2-oxoindolin-3-ylideneamino)-2-(thiophen-2-yl)quinazolin-4(3H)-one (**6g**).* Yield (62%); m.p. > 300 °C; IR *ν* 3306 (NH), 1708, 1681 (2C=O) cm^{-1}; ^1H NMR (DSMO-d_6) *δ* 7.01–8.11 (m, 10H, ArH); ^{13}C NMR (DSMO-d_6) *δ* 119.3, 120.6, 122.5, 123.3, 125.4, 126.3, 127.1, 127.6, 128.3, 129.5, 130.2, 131.6, 132.3, 133.5, 144.7, 148.1, 159.6, 161.8, 166.5; MS *m/z* (Rel. Int.) 406 (M^+, 29). Anal. ($C_{20}H_{11}ClN_4O_2S$, 406.4) C, 59.04 (58.83); H, 2.73 (2.57); N, 13.77 (13.52); S, 7.88 (7.61).

*4.1.3.8. (Z)-3-(5-Methyl-2-oxoindolin-3-ylideneamino)-2-(thiophen-2-yl)quinazolin-4(3H)-one (**6h**).* Yield (52%); m.p. 269–271 °C; IR ν 3301 (NH), 1700, 1689 (2C=O) cm^{-1}; ^1H NMR (DSMO-d_6) *δ* 2.37 (s, 3*H*, CH_3), 7.0–8.16 (m, 10H, ArH); ^{13}C NMR (DSMO-d_6) *δ* 25.1, 117.5, 120.7, 121.3, 122.6, 125.2, 126.8, 127.3, 127.7, 128.2, 129.8, 131.5, 132.1, 133.4, 134.7, 143.1, 147.4, 159.8, 162.0, 166.9; MS *m/z* (Rel. Int.) 386 (M^+, 35). Anal. ($C_{21}H_{14}N_4O_2S$, 386.43) C, 65.27 (64.99); H, 3.65 (3.34); N, 14.50 (14.68); S, 8.30 (8.52).

*4.1.3.9. (Z)-3-(5-Methoxy-2-oxoindolin-3-ylideneamino)-2-(thiophen-2-yl)quinazolin-4(3H)-one (**6i**).* Yield (47%); m.p. 285–287 °C; IR *ν* 3317 (NH), 1702, 1684 (2C=O) cm^{-1}; ^1H NMR (DSMO-d_6) *δ* 3.81 (s, 3*H*, OCH_3), 7.01–8.15 (m, 10H, ArH); ^{13}C NMR (DSMO-d_6) *δ* 55.3, 114.0, 116.3, 119.1, 120.4, 122.5, 122.7, 125.3, 126.1, 127.2, 127.6, 128.1, 132.5, 133.1, 139.4, 147.1, 157.0, 159.7, 162.3, 167.5; MS *m/z* (Rel. Int.) 402 (M^+, 38). Anal. ($C_{21}H_{14}N_4O_3S$, 402.43) C, 62.68 (62.41); H, 3.51 (3.35); N, 13.92 (14.22); S, 7.97 (8.15).

*4.1.3.10. (Z)-3-(5-Nitro-2-oxoindolin-3-ylideneamino)-2-(thiophen-2-yl)quinazolin-4(3H)-one (**6j**).* Yield (51%); m.p. 294–296 °C; IR *ν* 3309 (NH), 1705, 1687 (2C=O) cm–1; ^1H NMR (DSMO-d_6) *δ* 6.97–8.15 (m, 10H, ArH); ^{13}C NMR (DSMO-d_6) *δ* 118.3, 120.7, 122.1, 122.5, 123.2, 124.5, 125.4, 126.1, 127.0, 127.5, 128.3, 132.6, 133.5, 145.1, 147.5, 153.1, 159.6, 161.6, 167.2; MS *m/z* (Rel. Int.) 417 (M^+, 36). Anal. ($C_{20}H_{11}N_5O_4S$, 417.40) C, 57.55 (57.37); H, 2.66 (2.45); N, 16.78 (16.55); S, 7.68 (7.83).

4.2. Anti-proliferative activity

4.2.1. Materials

4.2.1.1. Chemicals and supplies. MTT (3-[4,5-dimethylthiazol-2-yl]-2,5-diphenyltetrazolium bromide) was purchased from Sigma Aldrich (St Louis, MO, USA). DMEM/high glucose, FBS and penicillin/streptomycin were obtained from Gibco (Grand Island, NY, USA).

4.2.1.2. Cell lines. Five human tumor cell lines were utilized in this study, namely medulloblastoma (Daoy and UW228-2), hepatocellular carcinoma (Huh-7), cervical carcinoma (Hela) and breast carcinoma (MDA-MB231). The routine maintenance and culture conditions for Daoy and UW228-2, HeLa and MDA-MB-231 cells have been previously described [17,28,29]. The hepatic cancer Huh-7 cells were kindly provided by Dr. Kezhong Zhang, Center for Cellular and Molecular Genetics, Wayne State University, Detroit, MI, and were maintained essentially as described [30]. Daoy and UW228-2 were cultured in DMEM/F12 supplemented with 10% FBS, 2 mM L-glutamine and 1% penicillin/streptomycin. Huh-7, Hela and

MDA-MB231 cells were grown in DMEM/high glucose supplemented with 10% FBS, 2 mM L-glutamine and 1% penicillin/streptomycin.

4.2.2. Methods

4.2.2.1. Screening of antiproliferative activity of the compounds by MTT assay. The new compounds were evaluated in a primary five cell line-one concentration (25 μg/ml) anticancer assay against the previously mentioned cell lines. The cytotoxic effect of the newly synthesized compounds was evaluated by testing the capacity of the reducing enzymes present in viable cells to convert MTT to formazan crystals as previously described [28,30], with some modifications. Briefly, cells cultured in complete medium were seeded into 96-well microtiter plates (in quintuplicates) with 2×10^4 cells per well and incubated at 37 °C under a humidified atmosphere of 5% CO_2 for 24 h. The cell medium in test wells were then changed to serum free medium (SFM) containing 25 μg/ml of the test compounds, while the cell medium in control wells were changed to SFM containing an equivalent volume of solvent (dimethyl sulfoxide "DMSO"). After incubation at 37 °C for 24 h, SFM in control and test wells were replaced by 100 μL/well of MTT; 0.5 mg/mL) in Phosphate-buffered saline (PBS) and incubated at 37 °C for an additional 3 h. MTT solution were removed and the purple formazan crystals formed at the bottom of the wells were dissolved using 100 μl isopropyl alcohol/well with shaking for 1 h at room temperature. The absorbance at 549 nm was read on a microplate reader (ELX 800; Bio-Tek Instruments, Winooski, VT, USA).

The dose response curves of the compounds effecting ≥50% inhibition in one-dose prescreening for each cell line were established with concentrations of 25, 12.5, 6.25, 3.125, 1.56 and 0.78 μg/mL, and the concentrations causing 50% cell growth inhibition (IC_{50}) were calculated. The cytotoxic activity of the (CFM-1) has previously been established in our laboratory as an inhibitor of tumor growth [16], against the five cell lines was examined at the same concentrations of tested compounds and utilized as a standard for comparative purposes.

Acknowledgment

This work was supported by a grant from the National Plan of Science, Technology and Innovation (Grant No.10-MED1188-02) King Saud University, Riyadh, Saudi Arabia., and the US Department of Veterans review grant (AKR).

Appendix A. Supplementary data

Supplementary data related to this article can be found at http://dx.doi.org/10.1016/j.ejmech.2014.12.048.

References

[1] P.A. Ganz, Cancer treatment and cognitive function: chemotherapy is not the only culprit, Oncol. (Willist. Park) 28 (2014) pii: 201378.
[2] (a) A. Garofalo, L. Goossens, B. Baldeyrou, A. Lemoine, S. Ravez, P. Six, M.H. David-Cordonnier, J.P. Bonte, P. Depreux, A. Lansiaux, J.F. Goossens, Design, synthesis, and DNA-binding of N-alkyl(anilino)quinazoline derivatives, J. Med. Chem. 53 (2010) 8089–8103;
(b) I. Khan, A. Ibrar, N. Abbas, A. Saeed, Recent advances in the structural library of functionalized quinazoline and quinazolinone scaffolds: synthetic approaches and multifarious applications, Eur. J. Med. Chem. 76 (2014) 193–244;
(c) X. Wang, J. Yin, L. Shi, G. Zhang, B. Song, Design, synthesis, and antibacterial activity of novel Schiff base derivatives of quinazolin-4(3*H*)-one, Eur. J. Med. Chem. 77 (2014) 65–74.
[3] J. Li, Y. Meng, Y. Liu, Z.Q. Feng, X.G. Chen, F84, a quinazoline derivative, exhibits high potent antitumor activity against human gynecologic malignancies, Investig. New Drugs 28 (2010) 132–138.
[4] D.W. Fry, A.J. Kraker, A. McMichael, L.A. Ambroso, J.M. Nelson, W.R. Leopold, R.W. Connors, A.J. Bridges, A specific inhibitor of the epidermal growth factor receptor tyrosine kinase, Science 265 (1994) 1093–1095.
[5] D.H. Boschelli, 4-anilino-3-quinolinecarbonitriles: an emerging class of kinase inhibitors, Curr. Top. Med. Chem. 2 (2002) 1051–1063.
[6] M. Bos, J. Mendelsohn, Y.M. Kim, J. Albanell, D.W. Fry, J. Baselga, PD153035, a tyrosine kinase inhibitor, prevents epidermal growth factor receptor activation and inhibits growth of cancer cells in a receptor number-dependent manner, Clin. Cancer Res. Off. J. Am. Assoc. Cancer Res. 3 (1997) 2099–2106.
[7] H. Kurokawa, C.L. Arteaga, Inhibition of erbB receptor (HER) tyrosine kinases as a strategy to abrogate antiestrogen resistance in human breast cancer, Clin. Cancer Res. Off. J. Am. Assoc. Cancer Res. 7 (2001) 4436s–4442s.
[8] L. Sun, C. Liang, S. Shirazian, Y. Zhou, T. Miller, J. Cui, J.Y. Fukuda, J.Y. Chu, A. Nematalla, X. Wang, H. Chen, A. Sistla, T.C. Luu, F. Tang, J. Wei, C. Tang, Discovery of 5-[5-fluoro-2-oxo-1,2-dihydroindol-(3Z)-ylidenemethyl]-2,4-dimethyl-1*H*-pyrrole-3-carboxylic acid (2-diethylaminoethyl)amide, a novel tyrosine kinase inhibitor targeting vascular endothelial and platelet-derived growth factor receptor tyrosine kinase, J. Med. Chem. 46 (2003) 1116–1119.
[9] R.R. Khanwelkar, G.S. Chen, H.C. Wang, C.W. Yu, C.H. Huang, O. Lee, C.H. Chen, C.S. Hwang, C.H. Ko, N.T. Chou, M.W. Lin, L.M. Wang, Y.C. Chen, T.H. Hseu, C.N. Chang, H.C. Hsu, H.C. Lin, Y.C. Shih, S.H. Chou, H.W. Tseng, C.P. Liu, C.M. Tu, T.L. Hu, Y.J. Tsai, J.W. Chern, Synthesis and structure-activity relationship of 6-arylureido-3-pyrrol-2-ylmethylideneindolin-2-one derivatives as potent receptor tyrosine kinase inhibitors, Bioorg. Med. Chem. 18 (2010) 4674–4686.
[10] D.Y. Heng, C. Kollmannsberger, Sunitinib, recent results in cancer research. Fortschritte der Krebsforschung, Progres rech. cancer 184 (2010) 71–82.
[11] L. Sun, N. Tran, F. Tang, H. App, P. Hirth, G. McMahon, C. Tang, Synthesis and biological evaluations of 3-substituted indolin-2-ones: a novel class of tyrosine kinase inhibitors that exhibit selectivity toward particular receptor tyrosine kinases, J. Med. Chem. 41 (1998) 2588–2603.
[12] A. Stopeck, M. Sheldon, M. Vahedian, G. Cropp, R. Gosalia, A. Hannah, Results of a phase I dose-escalating study of the antiangiogenic agent, SU5416, in patients with advanced malignancies, Clin. Cancer Res. Off. J. Am. Assoc. Cancer Res. 8 (2002) 2798–2805.
[13] A.D. Laird, P. Vajkoczy, L.K. Shawver, A. Thurnher, C. Liang, M. Mohammadi, J. Schlessinger, A. Ullrich, S.R. Hubbard, R.A. Blake, T.A. Fong, L.M. Strawn, L. Sun, C. Tang, R. Hawtin, F. Tang, N. Shenoy, K.P. Hirth, G. McMahon, Cherrington, SU6668 is a potent antiangiogenic and antitumor agent that induces regression of established tumors, Cancer Res. 60 (2000) 4152–4160.
[14] A.K. Rishi, L. Zhang, M. Boyanapalli, A. Wali, R.M. Mohammad, Y. Yu, J.A. Fontana, J.S. Hatfield, M.I. Dawson, A.P. Majumdar, U. Reichert, Identification and characterization of a cell cycle and apoptosis regulatory protein-1 as a novel mediator of apoptosis signaling by retinoid CD437, J. Biol. Chem. 278 (2003) 33422–33435.
[15] A.K. Rishi, L. Zhang, Y. Yu, Y. Jiang, J. Nautiyal, A. Wali, J.A. Fontana, E. Levi, A.P. Majumdar, Cell cycle- and apoptosis-regulatory protein-1 is involved in apoptosis signaling by epidermal growth factor receptor, J. Biol. Chem. 281 (2006) 13188–13198.
[16] J.H. Kim, C.K. Yang, K. Heo, R.G. Roeder, W. An, M.R. Stallcup, CCAR1, a key regulator of mediator complex recruitment to nuclear receptor transcription complexes, Mol. Cell 31 (2008) 510–519.
[17] V.T. Puliyappadamba, W. Wu, D. Bevis, L. Zhang, L. Polin, R. Kilkuskie, R.L. Finley Jr., S.D. Larsen, E. Levi, F.R. Miller, A. Wali, A.K. Rishi, Antagonists of anaphase-promoting complex (APC)-2-cell cycle and apoptosis regulatory protein (CARP)-1 interaction are novel regulators of cell growth and apoptosis, J. Biol. Chem. 286 (2011) 38000–38017.
[18] C.G. Wermuth, The Practice of Medicinal Chemistry, third ed., Academic Press, London, 2008.
[19] H.P.H.A. Frisch, R.D. Dennington II, T.A. Keith, J. Millam, B. Nielsen, A.J. Holder, J. Hiscocks, GaussView Version 5.0.8, Gaussian, Inc., Wallingford, CT, USA, 2009.
[20] A.D. Becke, Density-functional thermochemistry. III. The role of exact exchange, J. Chem. Phys. 98 (1993) 5648–5652.
[21] C. Lee, W. Yang, R.G. Parr, Development of the Colle-Salvetti correlation-energy formula into a functional of the electron density, Phys. Rev. B Condens. Matter 37 (1988) 785–789.
[22] B. Miehlich, A. Savin, H. Stoll, H. Preuss, Results obtained with the correlation-energy density functionals of Becke and Lee, Yang and Parr, Chem. Phys. Lett. 157 (1989) 200–206.
[23] G.W.T.M.J. Frisch, H.B. Schlegel, G.E. Scuseria, M.A. Robb, J.R. Cheeseman, G. Scalmani, V. Barone, B. Mennucci, G.A. Petersson, H. Nakatsuji, M. Caricato, X. Li, H.P. Hratchian, A.F. Izmaylov, J. Bloino, G. Zheng, J.L. Sonnenberg, M. Hada, M. Ehara, K. Toyota, R. Fukuda, J. Hasegawa, M. Ishida, T. Nakajima, Y. Honda, O. Kitao, H. Nakai, T. Vreven, J.A. Montgomery Jr., J.E. Peralta, F. Ogliaro, M. Bearpark, J.J. Heyd, E. Brothers, K.N. Kudin, V.N. Staroverov, R. Kobayashi, J. Normand, K. Raghavachari, A. Rendell, J.C. Burant, S.S. Iyengar, J. Tomasi, M. Cossi, N. Rega, J.M. Millam, M. Klene, J.E. Knox, J.B. Cross, V. Bakken, C. Adamo, J. Jaramillo, R. Gomperts, R.E. Stratmann, O. Yazyev, A.J. Austin, R. Cammi, C. Pomelli, J.W. Ochterski, R.L. Martin, K. Morokuma, V.G. Zakrzewski, G.A. Voth, P. Salvador, J.J. Dannenberg, S. Dapprich, A.D. Daniels, O. Farkas, J.B. Foresman, J.V. Ortiz, J. Cioslowski, D.J. Fox, Gaussian 09W, Revision A.1, Gaussian, Inc, Wallingford, CT, USA, 2009.
[24] I.V. Tetko, J. Gasteiger, R. Todeschini, A. Mauri, D. Livingstone, P. Ertl, V.A. Palyulin, E.V. Radchenko, N.S. Zefirov, A.S. Makarenko, V.Y. Tanchuk, V.V. Prokopenko, Virtual computational chemistry laboratory–design and description, J. Comput. Aided Mol. Des. 19 (2005) 453–463.

[25] 1115 NW, 4th Street, Gainesville, FL 32601, HyperChem (Molecular Modeling System), Hypercube, Inc., USA, 2007.
[26] D.M. Hawkins, S.C. Basak, D. Mills, Assessing model fit by cross-validation, J. Chem. Inf. Comput. Sci. 43 (2003) 579–586.
[27] IBM SPSS, Statistics for Windows, IBM Corp, Armonk, NY, USA, 2012.
[28] A.E. Ashour, S. Jamal, V.T. Cheryan, M. Muthu, K.M. Zoheir, A.M. Alafeefy, A.R. Abd-Allah, E. Levi, A.L. Tarca, L.A. Polin, A.K. Rishi, CARP-1 functional mimetics: a novel class of small molecule inhibitors of medulloblastoma cell growth, PloS One 8 (2013) e66733.
[29] C. Zhang, G. Wang, Z. Zheng, K.R. Maddipati, X. Zhang, G. Dyson, P. Williams, S.A. Duncan, R.J. Kaufman, K. Zhang, Endoplasmic reticulum-tethered transcription factor cAMP responsive element-binding protein, hepatocyte specific, regulates hepatic lipogenesis, fatty acid oxidation, and lipolysis upon metabolic stress in mice, Hepatology 55 (2012) 1070–1082.
[30] C. Kohle, O.A. Badary, K. Nill, B.S. Bock-Hennig, K.W. Bock, Serotonin glucuronidation by Ah receptor- and oxidative stress-inducible human UDP-glucuronosyltransferase (UGT) 1A6 in Caco-2 cells, Biochem. Pharmacol. 69 (2005) 1397–1402.